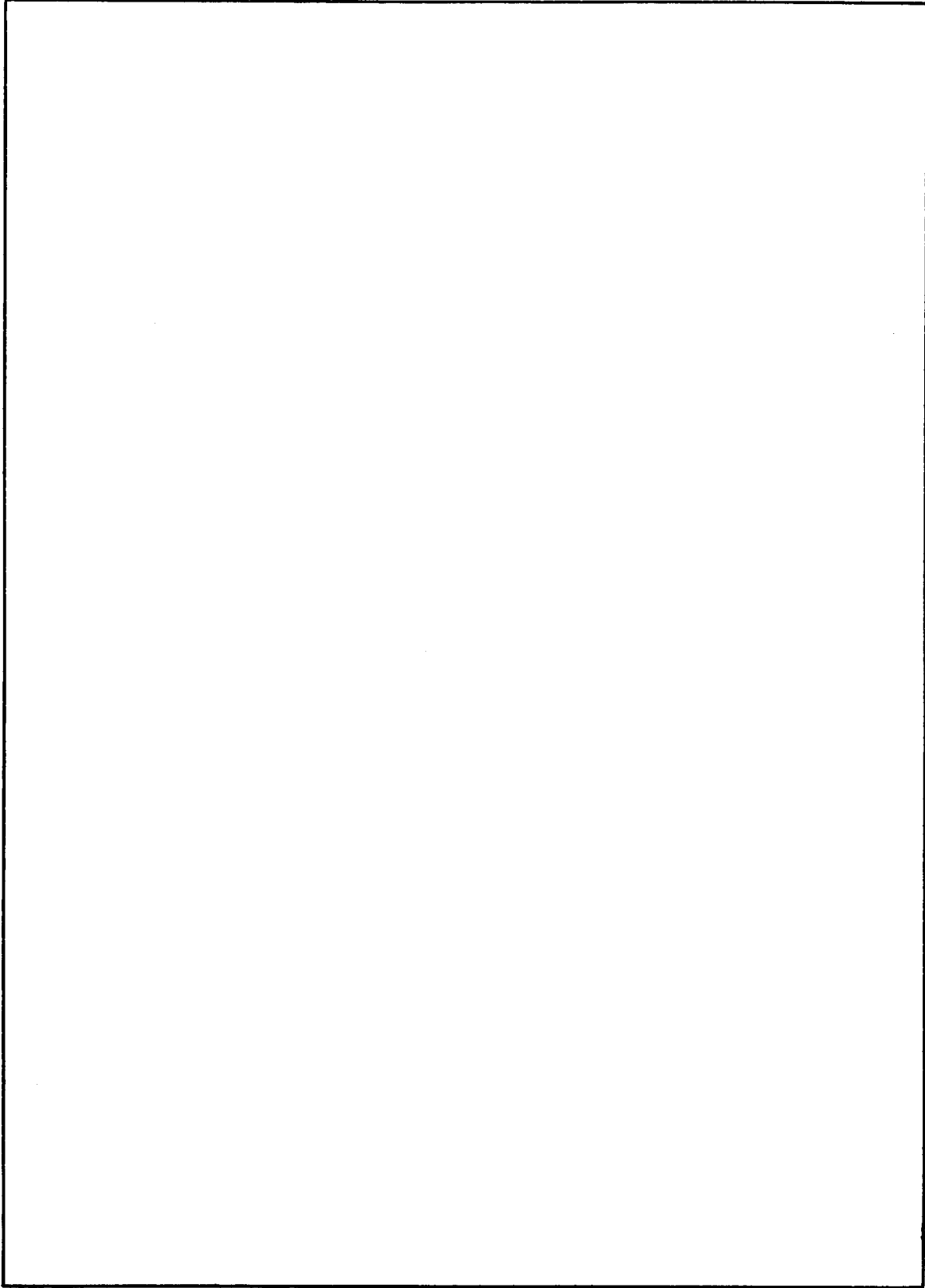


REPORT DOCUMENTATION PAGE		READ INSTRUCTIONS BEFORE COMPLETING FORM
1. REPORT NUMBER NRL Report 7675	2. GOVT ACCESSION NO.	3. RECIPIENT'S CATALOG NUMBER
4. TITLE (and Subtitle) Effects of the Anisotropic Elastic Modulus of a Boron-Fiber-Reinforced Aluminum-Matrix Composite on Specimens Calibrated for Crack-Length Determination		5. TYPE OF REPORT & PERIOD COVERED Final report on the NRL Problem.
		6. PERFORMING ORG. REPORT NUMBER
7. AUTHOR(s) A. M. Sullivan and J. Stoop		8. CONTRACT OR GRANT NUMBER(s)
9. PERFORMING ORGANIZATION NAME AND ADDRESS Naval Research Laboratory Washington, D.C. 20375		10. PROGRAM ELEMENT, PROJECT, TASK AREA & WORK UNIT NUMBERS NRL Problem M01-28 Project WR 022-04-001
11. CONTROLLING OFFICE NAME AND ADDRESS Department of the Navy Naval Air Systems Command Washington, D.C. 20360		12. REPORT DATE February 27, 1974
14. MONITORING AGENCY NAME & ADDRESS (if different from Controlling Office)		13. NUMBER OF PAGES 15
		15. SECURITY CLASS. (of this report) Unclassified
16. DISTRIBUTION STATEMENT (of this Report) Approved for public release; distribution unlimited.		15a. DECLASSIFICATION/DOWNGRADING SCHEDULE
17. DISTRIBUTION STATEMENT (of the abstract entered in Block 20, if different from Report)		
18. SUPPLEMENTARY NOTES		
19. KEY WORDS (Continue on reverse side if necessary and identify by block number) Fiber-reinforced metal-matrix composite Fracture-resistance parameter K_c Fracture resistance Anisotropy of Young's modulus Crack-Length determination		
20. ABSTRACT (Continue on reverse side if necessary and identify by block number) In an investigation undertaken to assess the suitability of the fracture mechanics parameter K_c for determining the fracture resistance of a boron-fiber-reinforced aluminum-matrix composite, calibration curves designed to measure crack length under load were prepared with specimens at various angles to the fiber axis of the sheet. The effect of the anisotropy of Young's modulus E is reflected in the curves obtained. Scatter in the data indicates that this is not a reliable method for determining crack length for this material, a boron-fiber/6061-aluminum composite.		
Manuscript submitted October 17, 1973.		

DD FORM 1473
1 JAN 73EDITION OF 1 NOV 65 IS OBSOLETE
S/N 0102-014-6601

i



CONTENTS

INTRODUCTION	1
EXPERIMENTAL PARAMETERS	1
Material	1
Specimen Preparation	2
Testing Procedure	3
DATA ANALYSIS	4
EXPERIMENTAL RESULTS	5
Young's Modulus	5
Unidirectional Material—Angles to the Fiber Axis:	
0° , 15° , 30° , and 90°	5
Multidirectional Material—Angles to the Fiber Axis:	
0° and 90°	7
DISCUSSION	7
CONCLUSIONS	11
REFERENCES	11
SYMBOLS	12

EFFECTS OF THE ANISOTROPIC ELASTIC MODULUS OF A BORON-FIBER-REINFORCED ALUMINUM-MATRIX COMPOSITE ON SPECIMENS CALIBRATED FOR CRACK-LENGTH DETERMINATION

INTRODUCTION

Advanced composites such as the fiber-reinforced metal-matrix materials are of considerable interest in structural applications where high stiffness is required. However, in common with all structural elements, the fracture resistance of such materials, that is, the ability to withstand the deleterious effect of cracks, flaws, or notches, must be known to insure fail-safe design.

One measurement of fracture resistance is the linear-elastic fracture mechanics (LEFM) parameter designated as K_c which applies to thin-sheet material essentially under conditions of plane stress. Here an amount of crack growth occurs prior to instability and catastrophic fracture.

To determine the value of K_c at instability, both load and crack length must be known, since $K_c = \alpha\sqrt{af}2a/W$. One method for determining the crack length uses the amount of central crack opening (COD) under load. Normalized as $EB[COD]/P$, values are plotted vs relative crack length $2a/W$. From this calibration curve, the crack length $2a$ can be determined readily from values of $EB[COD]/P$ determined from the P -vs- COD records of any test.

However, in all materials previously studied, Young's modulus E was approximately constant in all directions. This is not true of composites. In the direction of the fiber axis, the modulus of the fiber dominates; normal to the fiber axis, the modulus of the matrix dominates. Since these variations in E affect the normalized curve, it seemed appropriate to explore the nature of the calibration curve at several angles to the fiber axis. The information obtained should indicate the suitability of this method for determining crack extensions in the fiber-reinforced metal-matrix composites.

EXPERIMENTAL PARAMETERS

Material

The material was a boron-fiber-reinforced metal-matrix composite made by Amercom:

Boron fiber: Avco, 5.6-mil diameter

Aluminum: 6061-0

50% by volume of fiber

A: Unidirectional—8 layer

Manuscript submitted October 17, 1973.

B: Multidirectional—8 layer

Fiber direction and sequence:

 $0^\circ, +45^\circ, -45^\circ, 90^\circ, 90^\circ, -45^\circ, +45^\circ, 0^\circ$

The panels were approximately 20 by 20 in. (50 by 50 cm) in size and 0.056 in. (0.14 cm) thick.

Specimen Preparation

The calibration specimens were 6 in. (15 cm) in length L , 1 in. (2.5 cm) in width W , and 0.056 in. (0.14 cm) in thickness B and were cut with a water-cooled diamond wheel, which exhibited rapid wear with this material. For loading in a 10K-capacity Instron testing machine, it was necessary to reinforce the specimen with doublers or end tabs (Fig. 1). These were attached to the specimen with Metalbond 1113 adhesive. To insure proper alignment, the assembly was positioned in a jig with steel dowels and clamped in place for curing (Fig. 2). The curing was done at 266°F (130°C) for 1 hr. The center cracks were put in after curing to insure axiility. These were made using an electric-discharge process, elox. The series of slits were 0.063 in. (0.16 cm) wide, with an included angle of 60° at the tip. Crack lengths were 0.1, 0.2, 0.3, 0.4, 0.5, and 0.6 in. (0.25, 0.5, 0.75, 1, 1.25, and 1.5 cm).

Four sets of test specimens were prepared from the unidirectional material with the longitudinal axis at angles to the fiber axis of 0° , 15° , 30° , and 90° . Only two sets of specimens were tested for the multidirectional sheet; the angles to the fiber axis of the surface layer were 0° and 90° .

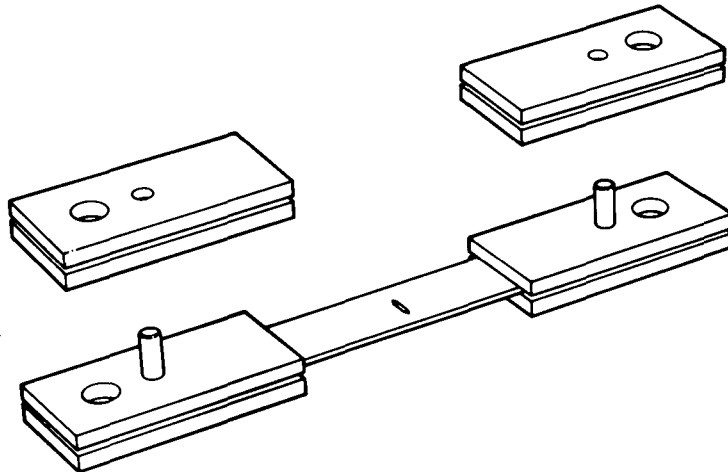


Fig. 1 — Doublers or end tabs used to reinforce a thin specimen for loading

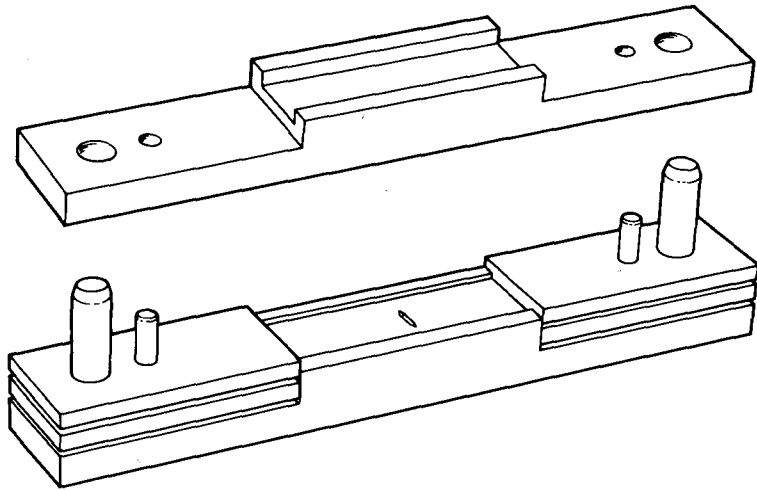


Fig. 2 — Jig for positioning the doublers and specimen in place with positioning dowels

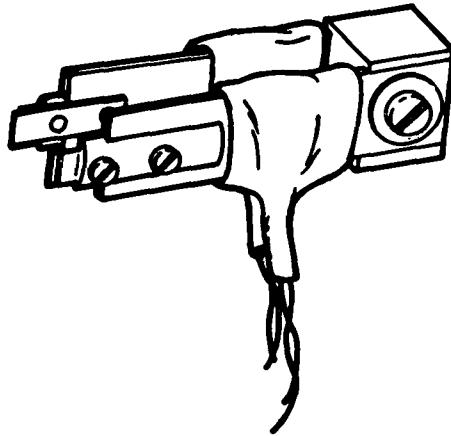


Fig. 3 — Strain-gage-instrumented probe together with the miniature tips angled to fit the knife edges on the specimen

Testing Procedure

The specimens were pin loaded through the doublers to clevises attached to the load train of the testing machine and subjected to elastic tensile extension (loads decreasing with lengthening cracks) at a head speed of 0.5 in./min. Crack opening was measured with a double-cantilever-beam gage (Fig. 3). Grooves at the ends of the beam arms contacted knife edges which were bolted to the specimen above and below the slot (Fig. 4). Load and crack opening were simultaneously graphed on a Hewlett-Packard XY Recorder. Since the panels were not absolutely flat and some warpage occurred during the double-specimen assembly process, it was found necessary to measure crack opening on both faces of the specimen. Each specimen was loaded and unloaded three times; angles of the slopes were measured and converted to a curve normalized as $EB[COD]/P$.

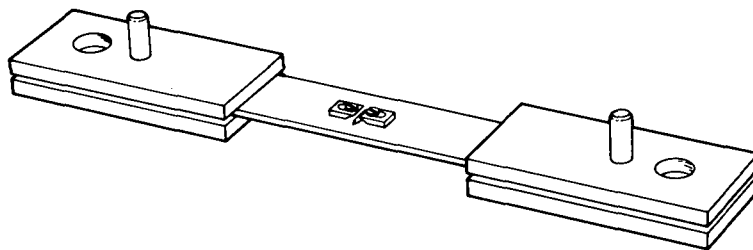


Fig. 4 — Specimen with the knife edges bolted in position

DATA ANALYSIS

Irwin's modification (1) of Westergaard's approach (2) to the problem of the stress field near a notch

$$\frac{E[COD]}{\sigma W} = 2 \left\{ \frac{2W}{\pi Y} \cosh^{-1} \left(\frac{\cosh \frac{\pi Y}{W}}{\cos \frac{\pi a}{W}} \right) - \frac{1 + \nu}{\left[1 + \left(\frac{\sin \frac{\pi a}{W}}{\sinh \frac{\pi Y}{W}} \right)^2 \right]^{1/2} + \nu} \right\} \frac{Y}{W} \quad (1)$$

has been shown applicable to displacements in the center-cracked tensile (CCT) specimen. Equation (1) is sensitive to gage span $2Y$ and specimen width W . Therefore, prior to testing the A1-B calibration series, calibration determinations were made on identical specimens of aluminum 7075-T6 and compared with the theoretical curve (Fig. 5). The experimental values indicate a greater degree of crack opening than anticipated. This trend has been noted previously (3, 4) by investigators using 3- and 4-in.-wide specimens, as is also seen in Fig. 5.

Young's modulus E was determined using a specimen without a central slot; a value of 10.4×10^6 psi was found for the aluminum alloy. Since this is in good agreement with reported values of E for this material determined in a more conventional manner, elastic moduli for the various testing directions of the A1-B composite were evaluated similarly:

$$E = \frac{0.400P}{B[COD]} \quad (2)$$

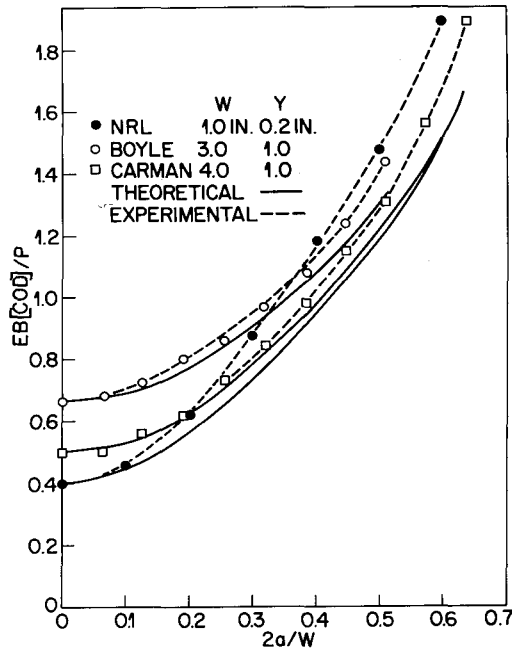


Fig. 5 — Normalized curve $EB[COD]/P$ vs $2a/W$ showing the theoretical curve and experimental data for two aluminum specimens of different width W , where the gage span $2Y = 2$ in. and for the A1-B specimen, where $W = 1.0$ in. and $2Y = 0.4$ in.

EXPERIMENTAL RESULTS

Young's Modulus

Values of Young's modulus E , determined in the manner previously described, are shown in Fig. 6. Comparison with other data (5) indicates good agreement. As expected, the multidirectional material has the same modulus in the 0° and 90° directions.

Unidirectional Material — Angles to the Fiber Axis: 0° , 15° , 30° , and 90°

The directions 0° , 15° , and 30° do not show too much discrepancy between values of $EB[COD]/P$ determined from measurements made on the (arbitrarily chosen) front and rear faces of the specimen (Fig. 7). As the angle increases, the curve lies lower. Thus at constant thickness B , load P , and $2a/W$, the stiffer directions indicate greatest COD . The transverse, 90° -angle data (Fig. 8) indicate greater disparity between the two faces; however, the average value (Fig. 9) is quite close to the 7075-T6 aluminum calibration curve. The differences are seen in Table 1. That the shapes of the curves differ can be noted in Fig. 10, where all are compared. The 90° -angle curve is clearly higher than the 30° -angle curve, as seen in Fig. 11.

SULLIVAN AND STOOP

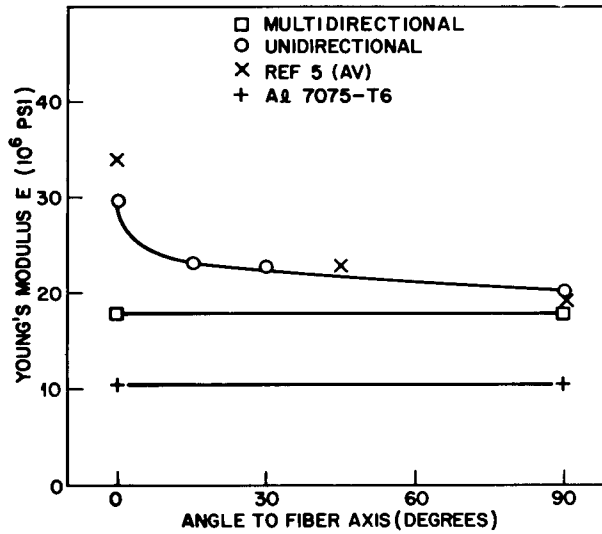


Fig. 6 — Young's Modulus E vs the specimen angle to the fiber axis

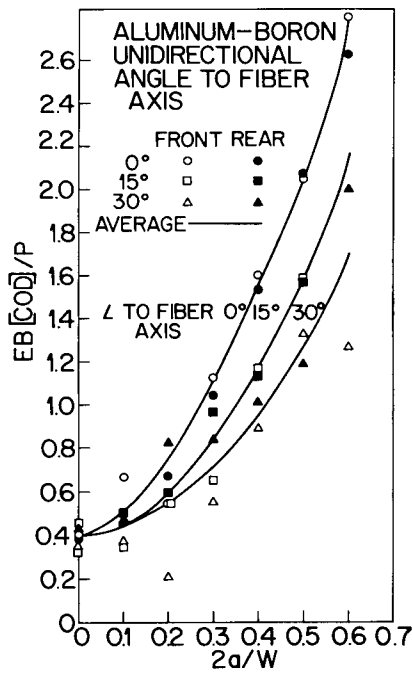


Fig. 7 — Normalized values of $EB[COD]/P$ for the unidirectional A1-B composite at 0°, 15°, and 30° to the fiber axis vs $2a/W$. The data are values on the front and rear surfaces of the specimen; the curves are drawn through average values.

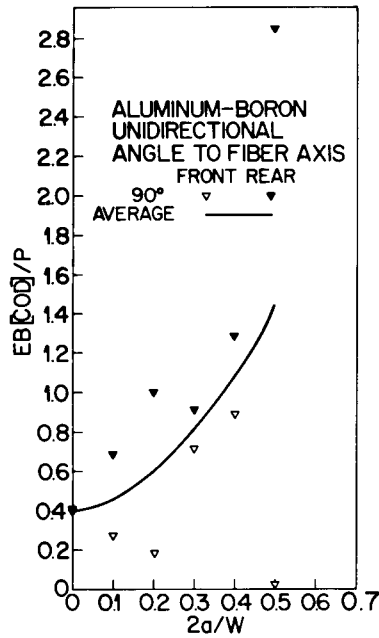


Fig. 8 — Normalized values of $EB[COD]/P$ for the unidirectional A1-B composite at 90° to the fiber axis vs $2a/W$. The data are values on the front and rear surfaces of the specimen; the curve is drawn through average values

Multidirectional Material — Angles to the Fiber Axis: 0° and 90°

Measurements on the two faces of these specimens differ widely (Fig. 12). However, averages differ by less than 5 percent except for the values at $2a/W = 0.5$ (Table 2). It is however surprising that they fall below the 7075-T6 aluminum curve, as did the unidirectional material in the 90° -angle direction.

DISCUSSION

Consideration of the results obtained from the cross-ply multidirectional material (where the fibers are symmetrically laid up with respect to the sheet plane and sheet thickness) leads to the conclusion that it behaves conventionally. The modulus E is isotropic, and in fact the $EB[COD]/P$ curve lies closer to the calculated theoretical curve than does the experimental curve for aluminum 7075-T6.

The fact that curves from the various axis and off-axis specimens of the unidirectional material do not normalize to a single curve, despite the fact that modulus values agree with those determined by other investigators, can only be rationalized by the assumption that an effect of the anisotropic modulus is predominating. Apparently the stiffer the material, the greater the crack opening. It could be argued that with the 0° specimens,

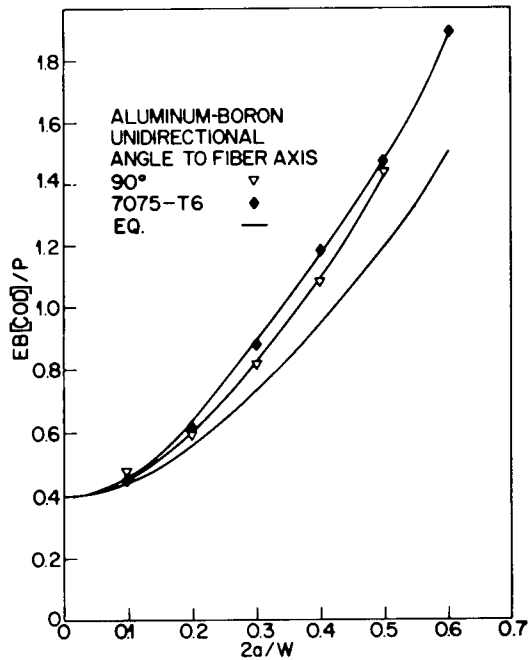


Fig. 9 — Normalized average values of $EB[COD]/P$ for the unidirectional $Al-B$ composite at 90° to the fiber axis vs $2a/W$ are compared with data from 7075-T6 aluminum and the calculated theoretical curve

Table 1
Percent Variation of $EB[COD]/P$ from a Value Averaged from 7075-T6 Aluminum and $Al-B$ (Unidirectional, at 90°)

$\frac{2a}{W}$	$\frac{EB[COD]}{P}$			
	Al	$Al-B$	Average Value	$\pm\%$
0	0.400	0.400	0.400	0
0.1	0.456	0.480	0.468	2.6
0.2	0.621	0.591	0.606	2.4
0.3	0.879	0.812	0.846	4.0
0.4	1.185	1.084	1.134	4.4
0.5	1.472	1.438	1.455	1.2
0.6	1.904	—	—	—

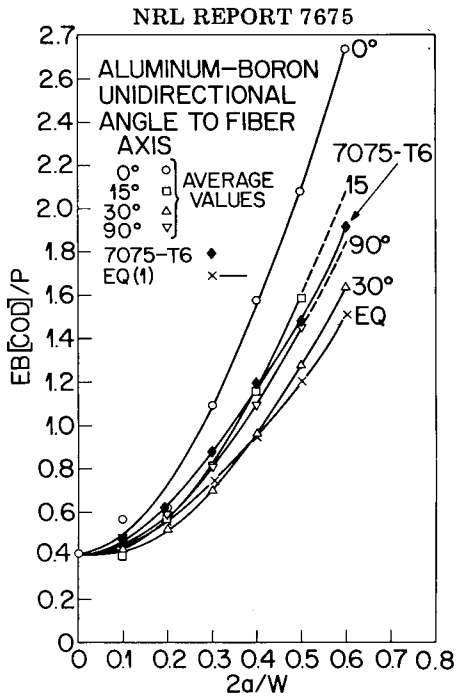


Fig. 10 — Normalized average values of $EB[COD]/P$ for the unidirectional $Al-B$ composite at 0° , 15° , 30° , and 90° to the fiber axis vs $2a/W$ are compared with data from 7075-T6 aluminum and the calculated theoretical curve

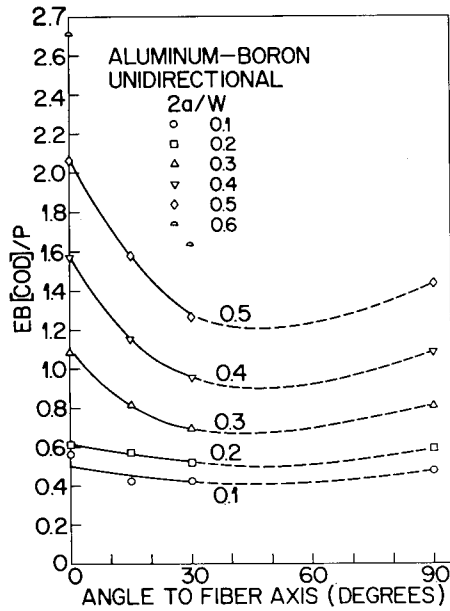


Fig. 11 — Normalized average values of $EB[COD]/P$ for the unidirectional $Al-B$ composite vs the angle to the fiber axis for a series of $2a/W$ values

SULLIVAN AND STOOP

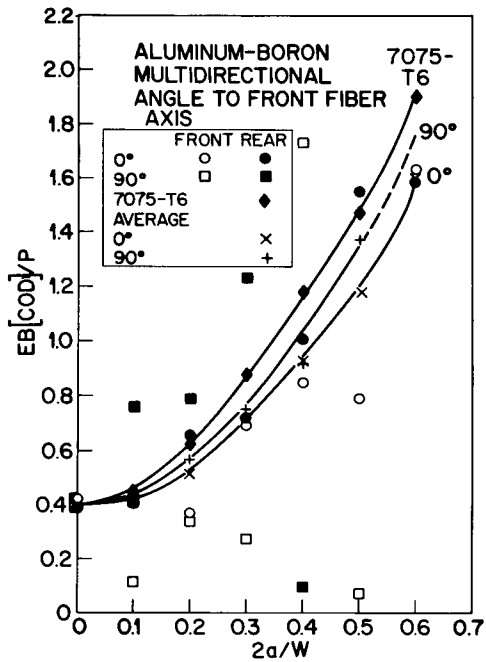


Fig. 12 — Normalized values of $EB[COD]/P$ for the multidirectional $Al-B$ composite at 0° and 90° to the surface fiber axis vs $2a/W$. The data are values on the front and rear surfaces of the specimen; the curves are drawn through average values. Data from 7075-T6 aluminum and the calculated theoretical curve are included for comparison

Table 2
Percent Variation of $EB[COD]/P$ from Averaged Values of $Al-B$ (Multidirectional 0° and 90°)

$\frac{2a}{W}$	$\frac{EB[COD]}{P}$			
	$Al-B$		Average Value	$\pm\%$
	0°	90°		
0	0.402	0.402	0.402	0
0.1	0.422	0.438	0.430	1.8
0.2	0.514	0.565	0.540	4.8
0.3	0.708	0.754	0.731	3.1
0.4	0.930	0.912	0.921	1.0
0.5	1.171	1.371	1.271	7.8
0.6	1.606	—	—	—

contraction in the low-modulus transverse direction forces the crack apart and that this effect diminishes as the angle to the fiber axis increases and the effects of the higher moduli are felt transversely. If this were so, in the transverse 90° specimens the effect of the high modulus should be most marked. The fact that the curve for the 90° specimens lies close to the aluminum curve suggests that unless some tractions are felt by the fiber axes, the effect is negligible in affecting the crack opening.

CONCLUSIONS

- The calibration curves reported here are not considered reliable for other than the 0° -angle specimen.
- Difficulties in calibrating are compounded by the narrowness of the specimen and the low loads required to insure elastic conditions in the low-strength aluminum matrix.
- Fracture resistance as measured by the fracture mechanics parameter K_c is unlikely to provide reliable characterization for the fiber-reinforced composite 6061 Al-B.

REFERENCES

1. G. R. Irwin, "Fracture Testing of High-Strength Sheet Materials Under Conditions Appropriate For Stress Analysis," NRL Report 5486, July 27, 1960.
2. H. M. Westergaard, "Bearing Pressures and Cracks," Trans. ASME, J. Appl. Mech. 6, A49 (1939).
3. R. W. Boyle, "A Method for Determining Crack Growth in Notched Stee Specimens," Materials Research and Standards 2, No. 8, 646 (1962).
4. C. M. Carman, D. F. Armiento, and H. Marcus, "Crack Resistance Properties of High Strength Aluminum Alloys," in *Proceedings of the First International Conference on Fracture* (Sendai, Japan), Vol. 2, Japanese Society for Strength and Fracture of Materials, Japan, 1966, p. 995.
5. D. A. Meyn and P. Shahinian, "Effect of Temperature and Strain Rate on the Tensile Properties of Aluminum-Boron, Epoxy-Boron, and Epoxy-Graphite Composites," NRL Memorandum Report 2609, June 1973.

SYMBOLS

a	Half crack length
B	Specimen thickness
COD	Crack-opening displacement
E	Young's modulus
K_c	Fracture-resistance parameter for plane stress
P	Load
W	Specimen width
Y	Half span of the displacement measuring gage
σ	Gross stress; load divided by the total area
ν	Poisson's ratio